On a Fictitious Domain Method for Flow and Wave Problems

M. O. Bristeau[1], V. Girault[2], R. Glowinski[3], T.-W Pan[4], J. Périaux[5], and Y. Xiang[1]

Summary

The main goal of this article is to discuss the application of a Lagrange multiplier based fictitious domain method to the solution of elliptic problems, then of the Navier-Stokes equations for incompressible viscous flow and finally of linear wave equations. This method is well suited to finite element approximations and takes advantage of the variational principles associated to large classes of partial differential problems. The results of numerical experiments validate this fictitious domain approach to the solution of partial differential equations with Dirichlet boundary conditions.

1 Introduction: Synopsis

Fictitious domain methods is a general term which covers in fact a large variety of solution methods for Partial Differential Equations; the literature on these methods is so large that we shall limit ourselves to [1]-[8] and the references therein. These methods are based however on the same following principle:

Suppose that one wants to solve the following boundary value problem

[1] INRIA, 78153 Le Chesnay, Paris, France
[2] Université P. et M. Curie, Paris, Toulouse, France
[3] Department of Mathematics, University of Houston, Houston, Texas 77204 USA, and Université P. et M. Curie, Paris, France
[4] Department of Mathematics, University of Houston, Houston, Texas 77204 USA
[5] Dassault Aviation, 92214 Saint–Cloud, France

Domain Decomposition Methods in Sciences and Engineering, edited by R. Glowinski *et al.*

$$A(u) = f \text{ in } \omega, \tag{1.1}$$
$$B(u) = g \text{ on } \gamma, \tag{1.2}$$

where in (1.1), (1.2), ω is (for simplicity) a bounded domain of $\boldsymbol{R}^d$, $\gamma = \partial\Omega$ is the boundary of ω, A and B are differential operators, and f, g are given functions. The idea is to *embed* ω in a larger domain Ω of very simple shape and to solve on Ω a problem whose solution $\tilde{u}$ satisfies

$$\tilde{u}|_\omega = u. \tag{1.3}$$

There is no miracle here since one has to take into account the boundary condition (1.2) in a way or another. Schematically we have boundary fitted fictitious domain methods (in which the finite element or finite difference mesh used to discretize the "extended problem" is locally distorted in the neighborhood of γ) or genuine fictitious domain methods in which the mesh used to discretize Ω is essentially independent of ω and γ.

In this article we shall concentrate on the second approach: it does not have the flexibility of general finite element methods, it is however well suited to the treatment of *Dirichlet boundary conditions* such as

$$u = g \text{ on } \gamma, \tag{1.4}$$

via *Lagrange multipliers*. The possibilities of this fictitious domain methodology will be illustrated by the numerical treatment of the following problems: *elliptic equations* in Section 2, the *Navier-Stokes equations* for incompressible viscous flow in Section 3 and the wave equation in Section 4.

2 Fictitious Domain Methods for Linear Dirichlet Problems

2.1 Formulation of a Model Problem

Let ω be a *bounded* domain of $\boldsymbol{R}^d$, we denote by $\gamma = \partial\Omega$ the boundary of ω. The problem under consideration is the *Dirichlet* problem defined by:

$$\alpha u - \nu\Delta u = f \text{ in } \omega, \tag{2.1}$$
$$u = g \text{ on } \gamma, \tag{2.2}$$

where, in (2.1), we have $\alpha \geq 0$ and $\nu > 0$.

2.2 A Fictitious Domain Formulation of the Dirichlet Problem (2.1), (2.2)

We follow the approach in [5]. We embed therefore ω in Ω as shown in Figure 1, below, and we denote by Γ the boundary of Ω. We assume that f and g are reasonably smooth (typically $f \in L^2(\omega)$ and $g \in H^{1/2}(\gamma)$).

It follows from [5] that problem (2.1), (2.2) is equivalent to the following saddle-point problem:

Find $\{\tilde{u}, \lambda\} \in V \times H^{-1/2}(\gamma)$ *such that*

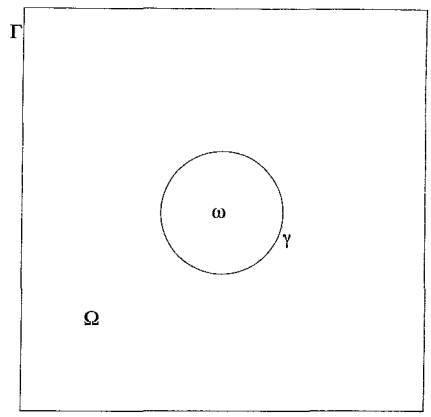

Figure 1. Embedding of ω

$$\int_\Omega (\alpha \tilde{u} v + \nu \nabla \tilde{u} \cdot \nabla v)\, dx = \int_\Omega \tilde{f} v\, dx + < \lambda, v >, \forall v \in V, \tag{2.3}$$

$$< \mu, \tilde{u} - g >= 0, \forall \mu \in H^{-1/2}(\gamma), \tag{2.4}$$

in the sense that $\tilde{u}|_\omega = u$; in (2.3), (2.4):

- $\tilde{f}$ denotes an $L^2(\Omega)$-extension of f such that $\tilde{f}|_\omega = f$;
- $< \cdot, \cdot >$ denotes the *duality pairing* between $H^{-1/2}(\gamma)$ and $H^{1/2}(\gamma)$ such that $< \mu, v >= \int_\gamma \mu v\, d\gamma$ if $\mu \in L^2(\gamma)$;
- V is either $H^1(\Omega)$, $H_0^1(\Omega)$, or $H_P^1(\Omega)$ where $H_P^1(\Omega)$ is the subspace of the functions of $H^1(\Omega)$ periodic at Γ.

Remark 2.1. The boundary "function" λ is a Lagrange multiplier associated with the boundary condition (2.2). Using Green's formula we can easily show that

$$\lambda = \nu \left[\frac{\partial \tilde{u}}{\partial \mathbf{n}}\right]\Big|_\gamma,$$

where $\left[\frac{\partial \tilde{u}}{\partial \mathbf{n}}\right]\Big|_\gamma$ denotes the jump of $\frac{\partial \tilde{u}}{\partial \mathbf{n}}$ at γ. □

Remark 2.2. If one uses penalty, we can approximate problems (2.1), (2.2) and (2.3), (2.4) by

Find $\tilde{u}_\epsilon \in V$ such that

$$\int_\Omega (\alpha \tilde{u}_\epsilon v + \nu \nabla \tilde{u}_\epsilon \cdot \nabla v)\, dx + \frac{1}{\epsilon} \int_\gamma \tilde{u}_\epsilon v\, d\gamma = \int_\Omega \tilde{f} v\, dx + \frac{1}{\epsilon} \int_\gamma g v\, d\gamma, \forall v \in V, \tag{2.5}$$

with $\epsilon > 0$. It follows from, e.g., [9, Appendix 1] that

$$\lim_{\epsilon \to 0} \|\tilde{u}_\epsilon - u\|_{H^1(\omega)} = 0.$$

One of the main drawbacks of the above approach is that after approximation the condition number of the discrete analogue of problem (2.5) deteriorates as $\epsilon \to 0$, *leading to an ill posed problem.* □

2.3 Iterative Solution of Problem (2.3), (2.4)

Problem (2.3) , (2.4) is a typical *linear saddle-point problem*; such problems can be solved by conjugate gradient variants of the Uzawa algorithm, like those discussed in, e.g., [5]. For the sake of completeness we shall describe such an algorithm. For simplicity, we assume that $\alpha > 0$. If $\tilde{u}$ is such that $\lambda \in L^2(\gamma)$, we can substitute this latter space to $H^{-1/2}(\gamma)$ in (2.3), (2.4) and solve the saddle-point problem by the following algorithm:

$$\lambda^0 \in L^2(\gamma) \text{ is given;} \tag{2.6}$$

solve

$$\text{Find } u^0 \in V \text{ such that}$$
$$\int_\Omega (\alpha u^0 v + \nu \nabla u^0 \cdot \nabla v)\, dx = \int_\Omega \tilde{f} v\, dx + \int_\gamma \lambda^0 v\, d\gamma,\ \forall v \in V, \tag{2.7}$$

and then

$$\text{Find } g^0 \in L^2(\gamma) \text{ such that}$$
$$\int_\gamma g^0 \mu\, d\gamma = \int_\gamma (u^0 - g)\mu\, d\gamma,\ \forall \mu \in L^2(\gamma), \tag{2.8}$$

and set

$$w^0 = g^0. \tag{2.9}$$

For $n \geq 0$, *assuming that* λ^n, g^n, w^n *are known, compute* $\lambda^{n+1}, g^{n+1}, w^{n+1}$, *as follows:*

solve

$$\text{Find } \bar{u}^n \in V \text{ such that}$$
$$\int_\Omega (\alpha \bar{u}^n v + \nu \nabla \bar{u}^n \cdot \nabla v)\, dx = \int_\gamma w^n v\, d\gamma,\ \forall v \in V, \tag{2.10}$$

$$\text{Find } \bar{g}^n \in L^2(\gamma) \text{ such that}$$
$$\int_\gamma \bar{g}^n \mu\, d\gamma = \int_\gamma \bar{u}^n \mu\, d\gamma,\ \forall \mu \in L^2(\gamma), \tag{2.11}$$

and compute

$$\rho_n = \int_\gamma |g^n|^2\, d\gamma \Big/ \int_\gamma w^n \bar{g}^n\, d\gamma, \tag{2.12}$$

and then

$$\lambda^{n+1} = \lambda^n - \rho_n w^n, \tag{2.13}$$
$$u^{n+1} = u^n - \rho_n \bar{u}^n, \tag{2.14}$$
$$g^{n+1} = g^n - \rho_n \bar{g}^n, \tag{2.15}$$

If $\|g^{n+1}\|_{L^2(\gamma)}/\|g^0\|_{L^2(\gamma)} \leq \epsilon$, *take* $\lambda = \lambda^{n+1}$, $\tilde{u} = u^{n+1}$; *if not compute*

$$\gamma_n = \|g^{n+1}\|^2_{L^2(\gamma)}/\|g^n\|^2_{L^2(\gamma)} \tag{2.16}$$

and update w^n *by*

$$w^{n+1} = g^{n+1} + \gamma_n w^n. \tag{2.17}$$

Do $n = n + 1$ *and go to* (2.10).

Remark 2.3. Relations (2.8) and (2.11) clearly imply that $g^0 = u^0|_\gamma - g$ *and* $\bar{g}^n = \bar{u}^n|_\gamma$, *respectively. We have chosen to write these solutions in integral form since this is better suited for the discrete problems where the discrete analogues of* g^n *and* $u^n|_\gamma$ *may live in different spaces.* □

Remark 2.4. Algorithm (2.6)-(2.17) is easy to implement; however we can not expect it to have optimal convergence properties since the natural space for λ *is not* $L^2(\gamma)$ *but* $H^{-1/2}(\gamma)$. *Iterating in this last space is more complicated, at least if* $\omega \subset \boldsymbol{R}^d$ *with* $d \geq 3$; *in the particular case where* $\omega \subset \boldsymbol{R}^2$ *we have shown in [5] that efficient iterative solvers can be obtained by preconditioning algorithm (2.6)-(2.17) (in fact its discrete analogue) by discrete variants of the boundary operator* $(\frac{\alpha}{\nu} I - \frac{d^2}{d\gamma^2})^{1/2}$ *(see [5] for implementation details).* □

2.4 Finite Element Approximation of Problem (2.3), (2.4)

We consider *two dimensional problems* only (for three dimensional application see ref. [6]). In order to discretize the saddle-point problem (2.3), (2.4) we need to approximate both spaces V and $H^{-1/2}(\gamma)$. Let us denote by h the pair $\{h_\Omega, h_\gamma\}$. To approximate V we introduce a *regular triangulation* $\mathcal{T}_h$ of Ω (as shown in Figure 2) with h_Ω the largest length of the edges of $\mathcal{T}_h$; then, we (classically) approximate V by

$$V_h = \{v_h | v_h \in V \cap C^0(\bar{\Omega}), v_h|_T \in P_1, \forall T \in \mathcal{T}_h\}, \tag{2.18}$$

with P_1 the space of the polynomials in 2 variables of degree ≤ 1. Concerning $H^{-1/2}(\gamma)$ we divide γ in subarcs of maximal length h_γ and denote by $\mathcal{A}_h$ the collection of these subarcs; we approximate then $H^{-1/2}(\gamma)$ (and also $L^2(\gamma)$) by

$$\Lambda_h = \{\mu_h |\, \mu_h|_a = constant, \forall a \in \mathcal{A}_h\}. \tag{2.19}$$

Remark 2.5. Let us insist on the fact that the extremities of the arcs of $\mathcal{A}_h$ *do not have to be at the intersection of* γ *with the edges of* $\mathcal{T}_h$ *(this can happen but it is not a necessity); actually we think that the partitioning of* γ *has to be mostly related to its intrinsic geometrical properties since this approach will facilitate the numerical treatment of those time dependent problems where* ω *(and therefore* γ*) is moving.* □

The saddle-point problem (2.3), (2.4) is approximated by the following finite dimensional saddle-point problem

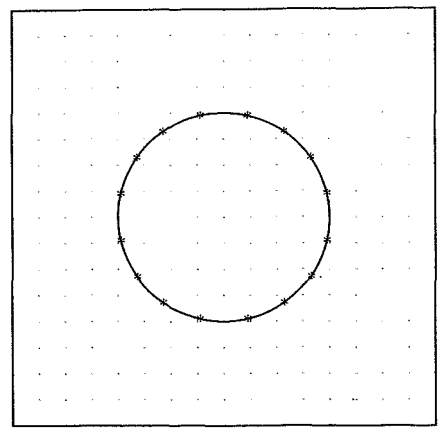

Figure 2. Visualization of $\mathcal{T}_h$ and $\mathcal{A}_h$

Find $\{u_h, \lambda_h\} \in V_h \times \Lambda_h$ *such that*

$$\int_\Omega (\alpha u_h v_h + \nu \nabla u_h \cdot \nabla v_h)\, dx = \int_\Omega \tilde{f} v_h\, dx + \int_\gamma \lambda_h v_h\, d\gamma,\ \forall v_h \in V_h, \tag{2.20}$$

$$\int_\gamma (u_h - g)\mu_h\, d\gamma = 0,\ \forall \mu_h \in \Lambda_h. \tag{2.21}$$

In the particular case where $g = 0$ it has been shown in [5] that

$$\lim_{h \to 0} u_h|_\omega = u \ \ in\ H^1(\omega), \tag{2.22}$$

where u is the solution of problem (2.1), (2.2); the convergence result (2.22) only requires that $\lim h_\Omega = \lim h_\gamma = 0$. In the cases where $g \neq 0$ it has been shown in [10] that

$$\lim_{h \to 0} \{u_h, \lambda_h\} = \{\tilde{u}, \lambda\} \ \ in\ H^1(\Omega) \times H^{-1/2}(\gamma) \tag{2.23}$$

if we assume that

$$c_1 h_\gamma \leq h_\Omega \leq c_2 h_\gamma, \tag{2.24}$$

with c_1 and c_2 well chosen positive numbers; actually in ref. [10] we shall also find a priori error estimates and values of c_1 and c_2 implying convergence.

To conclude this paragraph let us mention that numerical experiments for two and three dimensional test problems suggest (see [5] and [6]) that

$$\|u_h - u\|_{H^1(\omega)} \leq ch,$$
$$\|u_h - u\|_{L^\infty(\omega)} \leq ch^2,$$

which is better than the error estimates proved in [10].

Remark 2.5. It follows from (2.20), (2.21) that to obtain the linear system (associated to a symmetric indefinite matrix) equivalent to the above discrete saddle-point problem

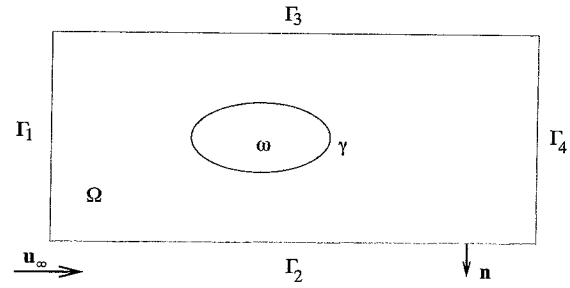

Figure 3.

we need the calculation of integrals like $\int_\gamma w_i \theta_k \, d\gamma$ *where* $\{w_i\}$ *(resp.,* $\{\theta_k\}$*) is a vector basis of* V_h *(resp.,* Λ_h*).* □

3 Application to the Solution of the Navier-Stokes Equations for Incompressible Viscous Fluids

3.1 Generalities. Problem Formulations

The fictitious domain solution of the Navier-Stokes equations modelling incompressible viscous fluids by methods generalizing those described in Section 2 has been discussed at length in [6]-[8], [11] (see also [12] where one applies this methodology to the simulation of three-dimensional visco-elastic flow). In the present article (of survey nature) we shall briefly discuss the fictitious domain solution of external flow like the one associated with Figure 3; indeed, such a flow is modelled by

$$\frac{\partial \mathbf{u}}{\partial t} - \nu \Delta \mathbf{u} + (\mathbf{u} \cdot \nabla)\mathbf{u} + \nabla p = \mathbf{f} \; in \; \Omega \setminus \bar{\omega}, \tag{3.1}$$

$$\nabla \cdot \mathbf{u} = 0 \; in \; \Omega \setminus \bar{\omega}, \tag{3.2}$$

$$\mathbf{u} = \mathbf{u}_\infty \; on \; \Gamma \setminus \Gamma_4, \; \mathbf{u} = \mathbf{0} \; on \; \gamma, \tag{3.3}$$

$$\nu \frac{\partial \mathbf{u}}{\partial \mathbf{n}} - \mathbf{n}p = \mathbf{0} \; on \; \Gamma_4, \tag{3.4}$$

$$\mathbf{u}(\mathbf{x}, 0) = \mathbf{u}_0(\mathbf{x}), \quad \mathbf{x} \in \Omega \setminus \bar{\omega}, (with \; \nabla \cdot \mathbf{u}_0 = 0). \tag{3.5}$$

In (3.1)-(3.5),

- $\Omega \setminus \bar{\omega}$ is the flow region,
- $\mathbf{u} = \{u_i\}_{i=1}^d$ denotes the velocity field,
- p is the pressure,
- $\nu (> 0)$ is a viscosity coefficient,
- $\mathbf{n}$ is the outer normal unit vector at $\partial\Omega$,
- $\mathbf{a} \cdot \mathbf{b} = \sum_{i=1}^d a_i b_i$, $\forall \, \mathbf{a} = \{a_i\}_{i=1}^d$, $\forall \, \mathbf{b} = \{b_i\}_{i=1}^d$,
- $(\mathbf{v} \cdot \nabla)\mathbf{w} = \{\sum_{j=1}^{j=d} v_j \frac{\partial w_i}{\partial x_j}\}_{i=1}^{i=d}$, $\forall \, \mathbf{v} = \{v_i\}_{i=1}^d$, $\forall \, \mathbf{w} = \{w_i\}_{i=1}^d$,

- $\mathbf{u}(0)$ denotes the function $\mathbf{x} \to \mathbf{u}(\mathbf{x}, 0)$; more generally, we shall denote by $\mathbf{u}(t)$ the function

$$\mathbf{x} \to \mathbf{u}(\mathbf{x}, t), \ \forall t \geq 0.$$

3.2 An Equivalent Fictitious Domain Formulation

The above Navier-Stokes problem is equivalent to the following *variational* system:

Find $\{\mathbf{U}(t), P(t), \lambda(t)\}$ *such that for almost every* $t > 0$, *we have*

$$\int_\Omega \mathbf{U}_t \cdot \mathbf{v}\, d\mathbf{x} + \nu \int_\Omega \nabla \mathbf{U} \cdot \nabla \mathbf{v}\, d\mathbf{x} + \int_\Omega (\mathbf{U} \cdot \nabla)\mathbf{U} \cdot \mathbf{v}\, d\mathbf{x} - \int_\Omega P \nabla \cdot \mathbf{v}\, d\mathbf{x}$$
$$= \int_\Omega \tilde{\mathbf{f}} \cdot \mathbf{v}\, d\mathbf{x} + \int_{\Gamma_1} \mathbf{g}_1 \cdot \mathbf{v}\, d\Gamma + \int_\gamma \lambda \cdot \mathbf{v}\, d\gamma, \ \forall \mathbf{v} \in \mathbf{V}_0, \tag{3.6}$$

$$\int_\gamma \mu \cdot \mathbf{U}\, d\gamma = 0, \ \forall \mu \in (L^2(\gamma))^d, \tag{3.7}$$

$$\int_\Omega q \nabla \cdot \mathbf{U}\, d\mathbf{x} = 0, \ \forall q \in L^2(\Omega), \tag{3.8}$$

$$\mathbf{U} = \mathbf{u}_\infty \ on \ \Gamma \setminus \Gamma_4, \tag{3.9}$$

$$\mathbf{U}(0) = \mathbf{U}_0, \ such \ that \ \nabla \cdot \mathbf{U}_0 = 0 \ in \ \Omega, \ \mathbf{U}_0|_{\Omega \setminus \bar{\omega}} = \mathbf{u}_0. \tag{3.10}$$

In (3.6) the space $\mathbf{V}_0$ is defined by

$$\mathbf{V}_0 = \{\mathbf{v} | \mathbf{v} \in (\mathbf{H}^1(\Omega))^d, \mathbf{v} = \mathbf{0} \ on \ \Gamma \setminus \Gamma_4\}. \tag{3.11}$$

In this context the equivalence between (3.1)-(3.5) and (3.6)-(3.10) means that $\mathbf{U}|_{\Omega \setminus \bar{\omega}} = \mathbf{u}$, $P|_{\Omega \setminus \bar{\omega}} = p$. We remind that we are here in a situation where the condition on Γ_4, namely (3.4), implies the *uniqueness* of the pressure associated to $\mathbf{u}$.

3.3 Time Discretization by Operator Splitting

Operator splitting algorithms like those discussed in, e.g., [13]-[16] (see also [17]) provide a systematic and elegant way to decouple the various difficulties associated with the solution of problem (3.6)-(3.10); the resulting schemes are described in [6]-[8], [11] and the scheme below is from these references. It is a particular application of the θ-scheme that we have introduced in [18], [19] and which combines good stability and accuracy properties (particularly if $\theta = 1 - 1/\sqrt{2}$). With $\Delta t > 0$ a time discretization step, this scheme takes the following form:

$$\mathbf{U}^0 = \mathbf{U}_0; \tag{3.12}$$

for $n \geq 0$, *knowing* $\mathbf{U}^n$, *find* $\{\mathbf{U}^{n+\theta}, P^{n+\theta}\}$, $\mathbf{U}^{n+1-\theta}$, *and* $\{\mathbf{U}^{n+1}, P^{n+1}\}$ *via*

$$\int_\Omega \frac{\mathbf{U}^{n+\theta} - \mathbf{U}^n}{\theta \Delta t} \cdot \mathbf{v}\, d\mathbf{x} + \alpha\nu \int_\Omega \nabla \mathbf{U}^{n+\theta} \cdot \nabla \mathbf{v}\, d\mathbf{x}$$
$$- \int_\Omega P^{n+\theta} \nabla \cdot \mathbf{v}\, d\mathbf{x} - \int_\gamma \lambda^{n+\theta} \cdot \mathbf{v}\, d\gamma \tag{3.13}_1$$

$$= \int_\Omega \tilde{\mathbf{f}}^{n+\theta} \cdot \mathbf{v}\, d\mathbf{x} - \int_\Omega (\mathbf{U}^n \cdot \nabla)\mathbf{U}^n \cdot \mathbf{v}\, d\mathbf{x} - \beta\nu \int_\Omega \nabla \mathbf{U}^n \cdot \nabla \mathbf{v}\, d\mathbf{x},\ \forall \mathbf{v} \in \mathbf{V}_0,$$

$$\int_\Omega \nabla \cdot \mathbf{U}^{n+\theta} q\, d\mathbf{x} = 0,\ \forall q \in L^2(\Omega), \tag{3.13}_2$$

$$\int_\gamma \mathbf{U}^{n+\theta} \cdot \mu = 0,\ \forall \mu \in (L^2(\gamma))^d, \tag{3.13}_3$$

$$\mathbf{U}^{n+\theta} = \mathbf{u}_\infty \ on\ \Gamma \setminus \Gamma_4; \tag{3.13}_4$$

$$\int_\Omega \frac{\mathbf{U}^{n+1-\theta} - \mathbf{U}^{n+\theta}}{(1-2\theta)\triangle t} \cdot \mathbf{v}\, d\mathbf{x} + \beta\nu \int_\Omega \nabla \mathbf{U}^{n+1-\theta} \cdot \nabla \mathbf{v}\, d\mathbf{x}$$
$$+ \int_\Omega (\mathbf{U}^{n+\delta} \cdot \nabla)\mathbf{U}^{n+1-\theta} \cdot \mathbf{v}\, d\mathbf{x} \tag{3.14}_1$$
$$= \int_\Omega \tilde{\mathbf{f}}^{n+1-\theta} \cdot \mathbf{v}\, d\mathbf{x} + \int_\gamma \lambda^{n+\theta} \cdot \mathbf{v}\, d\gamma + \int_\Omega P^{n+\theta} \nabla \cdot \mathbf{v}\, d\mathbf{x}$$
$$-\alpha\nu \int_\Omega \nabla \mathbf{U}^{n+\theta} \cdot \nabla \mathbf{v}\, d\mathbf{x},\ \forall \mathbf{v} \in \mathbf{V}_0,$$

$$\mathbf{U}^{n+1-\theta} = \mathbf{u}_\infty \ on\ \Gamma \setminus \Gamma_4; \tag{3.14}_2$$

and finally,

$$\int_\Omega \frac{\mathbf{U}^{n+1} - \mathbf{U}^{n+1-\theta}}{\theta\triangle t} \cdot \mathbf{v}\, d\mathbf{x} + \alpha\nu \int_\Omega \nabla \mathbf{U}^{n+1} \cdot \nabla \mathbf{v}\, d\mathbf{x}$$
$$- \int_\Omega P^{n+1} \nabla \cdot \mathbf{v}\, d\mathbf{x} - \int_\gamma \lambda^{n+1} \cdot \mathbf{v}\, d\gamma \tag{3.15}_1$$
$$= \int_\Omega \tilde{\mathbf{f}}^{n+1} \cdot \mathbf{v}\, d\mathbf{x} - \int_\Omega (\mathbf{U}^{n+1-\theta} \cdot \nabla)\mathbf{U}^{n+1-\theta} \cdot \mathbf{v}\, d\mathbf{x}$$
$$-\beta\nu \int_\Omega \nabla \mathbf{U}^{n+1-\theta} \cdot \nabla \mathbf{v}\, d\mathbf{x},\ \forall \mathbf{v} \in \mathbf{V}_0,$$

$$\int_\Omega \nabla \cdot \mathbf{U}^{n+1} q\, d\mathbf{x} = 0,\ \forall q \in L^2(\Omega), \tag{3.15}_2$$

$$\int_\gamma \mathbf{U}^{n+1} \cdot \mu = 0,\ \forall \mu \in (L^2(\gamma))^d, \tag{3.15}_3$$

$$\mathbf{U}^{n+1} = \mathbf{u}_\infty \ on\ \Gamma \setminus \Gamma_4. \tag{3.15}_3$$

In (3.12)-(3.15) we have taken $\alpha = (1-2\theta)/(1-\theta)$ and $\beta = \theta/(1-\theta)$. In relation $(3.14)_1$, δ is equal to either θ or $1-\theta$, the second choice making problem (3.14)

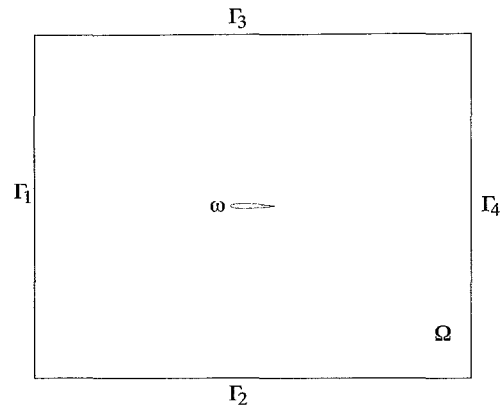

Figure 4.

nonlinear but increasing the stability of the scheme. We observe that the intermediate solution $\mathbf{U}^{n+1-\theta}$ is not required to satisfy the incompressibility condition and the no-slip condition on γ. The solution of the subproblems encountered in each time step is briefly discussed in the following paragraph.

3.4 Solution of the Subproblems

The solution of *advection-diffusion* problems such as (3.14) has been discussed at length in refs. [13]-[16]; we shall not return therefore on those topics. After discretization, problems (3.13) and (3.15) provide linear systems of the following form

$$\begin{cases} A\mathbf{U} + B^t P + C^t \lambda & = \mathbf{b}, \\ B\mathbf{U} & = \mathbf{c}, \\ C\mathbf{U} & = \mathbf{d}. \end{cases} \tag{3.16}$$

Problem (3.16) is a generaiized saddle-point problem. The solution of (3.16) has been discussed in [6]-[8], [11]; in ref. [11], in particular, we discuss a *one shot method*, of *conjugate gradient type*, which *simultaneously* adjusts the *incompressibility condition* $\nabla \cdot \mathbf{U} = 0$ in Ω and the *no-slip condition* $\mathbf{U} = \mathbf{0}$ on γ. The one shot method has good parallelization properties, but we think that there is still room for many improvements concerning the speed of convergence; in particular, we think, to apply to (3.16) the methods developed recently by Y. Kuznetsov for the fast solution of saddle-point problems (see [20]).

3.5 Numerical Experiments

We consider test problems where ω is a NACA0012 airfoil with zero degree and then 5 degrees angle of attack. The airfoil is centered at $(0,0)$ and its chord length is 0.35; finally ω is contained in Ω, where $\Omega = (-0.625, 0.625) \times (-0.5, 0.5)$ (see Figure 4). The boundary conditions are defined as follows:

$$\mathbf{u} = \mathbf{0}\, on\, \gamma,\ \mathbf{u} = (1 - e^{-ct})\{1,0\}\, on\, \Gamma_1 \cup \Gamma_2 \cup \Gamma_3 (= \Gamma \setminus \Gamma_4), \tag{3.17}$$

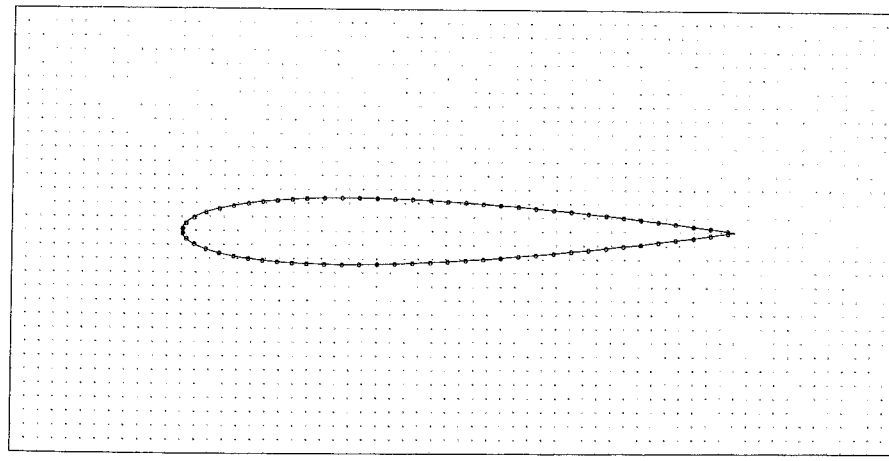

Figure 5. Mesh of γ where "o" are the mesh points on γ and part of the triangulation of Ω with meshsize $h = 1/128$.

$$\nu \frac{\partial \mathbf{u}}{\partial \mathbf{n}} - \mathbf{n}p = \mathbf{0} \, on \, \Gamma_4, \tag{3.18}$$

where c is a positive constant in (3.17).

As a finite dimensional subspace of $\mathbf{V}$, we choose

$$\mathbf{V}_h = \{\mathbf{v}_h | \mathbf{v}_h \in H^1_{0h} \times H^1_{0h}\}, \tag{3.19}$$

where

$$H^1_{0h} = \{\phi_h | \phi_h \in C^0(\bar{\Omega}), \phi_h|_T \in P_1, \ \forall T \in \mathcal{T}_h, \ \phi_h = 0 \, on \, \Gamma \backslash \Gamma_4\}, \tag{3.20}$$

with $\mathcal{T}_h$ a triangulation of Ω (see, e.g, Figure 5), P_1 the space of the polynomials in x_1, x_2 of degree ≤ 1. A traditional way of approximating the pressure is to take it in the space

$$H^1_{2h} = \{\phi_h | \phi_h \in C^0(\bar{\Omega}), \phi_h|_T \in P_1, \ \forall T \in \mathcal{T}_{2h}\}, \tag{3.21}$$

where $\mathcal{T}_{2h}$ is a triangulation twice coarser than $\mathcal{T}_h$. Concerning the space Λ_h approximating Λ, we define it by

$$\begin{aligned} \Lambda_h = \{\mu_h | \mu_h \in (L^\infty(\partial\omega))^2, \mu_h \, &is \, constant \, on \, the \, arc \, joining \\ &2 \, consecutive \, mesh \, points \, on \, \gamma\}. \end{aligned} \tag{3.22}$$

A particular choice for the mesh points on γ is shown on Figure 5. As a rule we have to put more mesh points at the leading edge; also mesh points have to be chosen carefully at the trailing edge. With a bad choice of mesh points on γ (e.g., a uniform mesh for a NACA0012), the Dirichlet boundary condition can not be matched very well for the case where the product $\nu \triangle t$ is of the order of 10^{-8}. The numerical

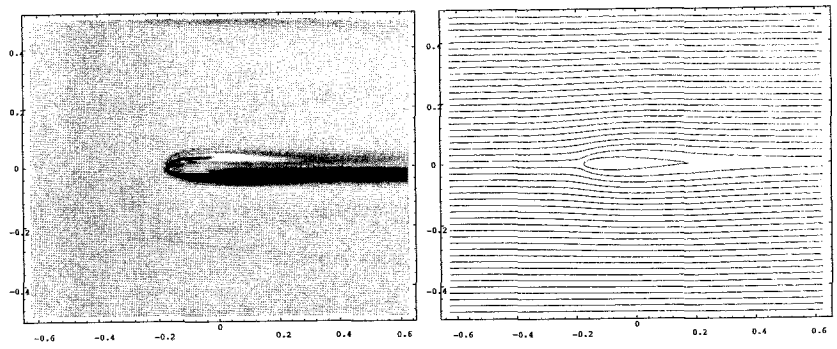

Figure 6. Vorticity density (left) and streamlines (right) for the flow past NACA0012 with zero degree angle of attack. Flow direction is from the left to the right, the Reynolds number is 1000, dimensionless time is 1.8.

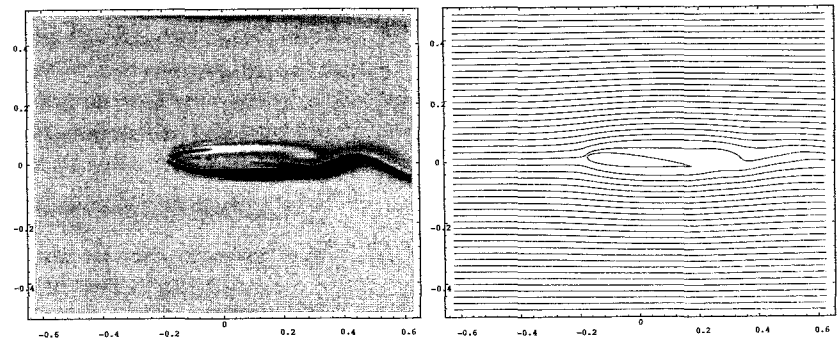

Figure 7. Vorticity density (left) and streamlines (right) for the flow past NACA0012 with 5 degrees angle of attack. Flow direction is from the left to the right, the Reynolds number is 1000, dimensionless time is 1.34.

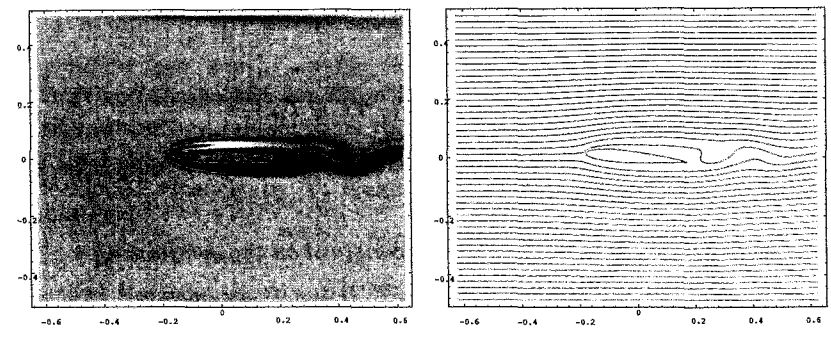

Figure 8. Vorticity density (left) and streamlines (right) for the flow past NACA0012 with 5 degrees angle of attack. Flow direction is from the left to the right, the Reynolds number is 1000, dimensionless time is 1.525.

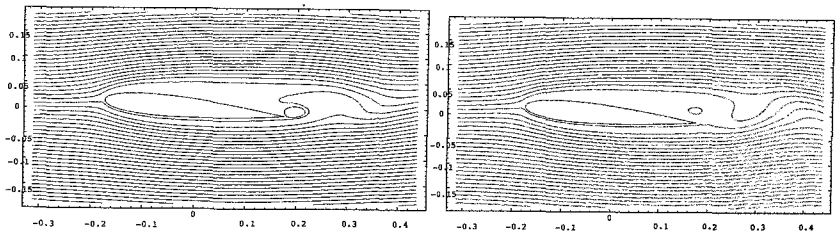

Figure 9. Local enlargement from Figures 7 (left) and 8 (right) of the streamlines distribution around NACA0012 with 5 degrees angle of attack.

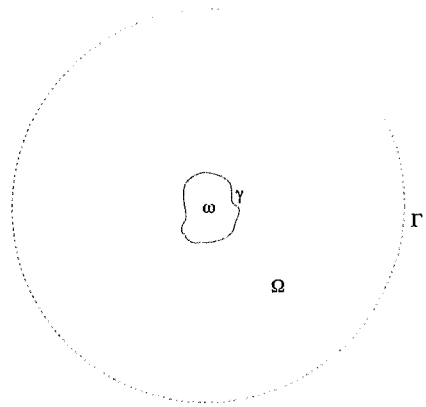

Figure 10

results presented here have been obtained for Re= 10^3 (taking the chord of the airfoil as characteristic length) with meshsizes $h_v = 1/256$ to approximate velocity and $h_p = 1/128$ to approximate pressure, time discretization step $\triangle t = 2.5 \times 10^{-3}$ and $c = 20$ in (3.17). In Figure 6 where the angle of attack is zero degree, the vorticity distribution and stream lines are almost symmetric with respect to the x_1 direction. For the case where the angle of attack is 5 degrees, *Von Kàrmàn vortex shedding* occurs (see Figures 7 and 8). The local enlargement of streamlines distribution around the airfoil is shown in Figure 9 for the 5 degrees incidence case.

4 Fictitious Domain Methods for Wave Problems

4.1 Formulation of a Model Wave Problem

We consider for simplicity a *wave equation* with constant coefficients but the method below can be generalized to variable coefficient wave equations and to systems such as the *Maxwell equations* and the *equations of Elasto-Dynamics*. The problem that we address is the solution of the *scattering* type problem associated with

$$\frac{\partial^2 u}{\partial t^2} - \Delta u = 0 \; in \; \Omega \setminus \bar{\omega}, \tag{4.1}$$

$$u = g \; on \; \gamma, \tag{4.2}$$

$$\frac{\partial u}{\partial t} + \frac{\partial u}{\partial \mathbf{n}} = 0 \; on \; \Gamma, \tag{4.3}$$

$$u(0) = u_0, \; \frac{\partial u}{\partial t}(0) = u_1. \tag{4.4}$$

The geometrical configuration is the one shown in Figure 10 where Ω is the larger domain in which ω has been embedded; actually $\Gamma(= \partial\Omega)$ will be used as an artificial boundary on which the (simple) *radiation condition* (4.3) has been specified.

4.2 A Fictitious Domain Equivalent Formulation of the Wave Problem (4.1)-(4.4)

Using, once again, a Lagrange multiplier approach it is fairly easy to show that problem (4.1)-(4.4) is equivalent to finding a pair $\{U, \lambda\}$ so that

$$\int_\Omega \frac{\partial^2 U}{\partial t^2} v \, d\mathbf{x} + \int_\Omega \nabla U \cdot \nabla v \, d\mathbf{x} + \int_\Gamma \frac{\partial U}{\partial t} v \, d\Gamma = \int_\gamma \lambda v \, d\gamma, \; \forall v \in H^1(\Omega), \tag{4.5}$$

$$\int_\gamma \mu (U - g) \, d\gamma = 0, \; \forall \mu \in L^2(\gamma), \tag{4.6}$$

$$U(0) = U_0, \; \frac{\partial U}{\partial t}(0) = U_1, \tag{4.7}$$

in the sense that $U|_{\Omega \setminus \bar{\omega}} = u$. The notation in (4.5), (4.6) is self-explanatory; in (4.7) U_0 and U_1 are well chosen extensions of u_0 and u_1, respectively (U_0 shall be a H^1-extension of u_0, while for u_1 a L^2-extension U_1 will be sufficient).

4.3 Space and Time Discretization of Problem (4.5)-(4.7)

Let us denote by V_h a finite dimensional finite element subspace of $H^1(\Omega)$ defined as follows:

$$V_h = \{v_h | v_h \in C^0(\bar{\Omega}), v_h|_T \in P_1, \; \forall T \in \mathcal{T}_h\}$$

with $\mathcal{T}_h$ a triangulation of Ω. Similarly we approximate $L^2(\gamma)$ by Λ_h, defined as in (3.22). We approximate then problem (4.5)-(4.7) by

$$\int_\Omega \frac{\partial^2 U_h}{\partial t^2} v_h \, d\mathbf{x} + \int_\Omega \nabla U_h \cdot \nabla v_h \, d\mathbf{x} + \int_\Gamma \frac{\partial U_h}{\partial t} v_h \, d\Gamma = \int_\gamma \lambda_h v_h \, d\gamma, \; \forall v_h \in V_h, \tag{4.8}$$

$$\int_\gamma \mu_h (U_h - g) \, d\gamma = 0, \; \forall \mu_h \in \Lambda_h, \tag{4.9}$$

$$U_h(0) = U_{0h}, \; \frac{\partial U_h}{\partial t}(0) = U_{1h}, \tag{4.10}$$

$$\{U_h(t), \lambda_h(t)\} \in V_h \times \Lambda_h \; for \; almost \; every \; t > 0. \tag{4.11}$$

Time discretizing problem (4.8)-(4.11) is quite easy, particularly if one uses the scheme below where we suppose that U_h^{n-1}, U_h^n are already known:

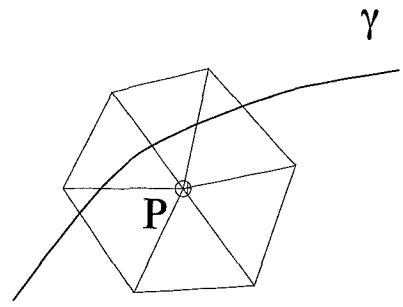

Figure 11

$$\int_\Omega \frac{U_h^{n+1} + U_h^{n-1} - 2U_h^n}{|\triangle t|^2} v_h \, d\mathbf{x} + \int_\Omega \nabla U_h^n \cdot \nabla v_h \, d\mathbf{x} \tag{4.12}$$
$$+ \int_\Gamma \frac{U_h^{n+1} - U_h^{n-1}}{2\triangle t} v_h \, d\Gamma = \int_\gamma \lambda_h^n v_h \, d\gamma, \ \forall v_h \in V_h,$$

$$\int_\gamma \mu_h (U_h^{n+1} - g^{n+1}) \, d\gamma = 0, \ \forall \mu_h \in \Lambda_h, \tag{4.13}$$

$$\{U_h^{n+1}, \lambda_h^n\} \in V_h \times \Lambda_h \ \forall n \geq 0, \tag{4.14}$$

$$U_h^0 = U_{0h}, \ U_h^1 - U_h^{-1} = 2\triangle t U_{1h}. \tag{4.15}$$

The above scheme is "almost" *explicit*; implicitness concerns only those values of U_h^{n+1} at the nodes of $\mathcal{T}_h$ whose associated shape function support intersects γ (as shown in Figure 11)

Assuming that we use the *trapezoidal rule* to compute the first and third integrals in the left hand side of (4.12), U_h^{n+1} and λ_h^n are obtained via the solution of a linear system of the following form

$$\begin{cases} A_h U_h + B_h^t \lambda_h = b_h, \\ B_h U_h \qquad\quad = c_h, \end{cases} \tag{4.16}$$

where A_h is a $N_h \times N_h$ symmetric and positive definite matrix (with N_h=dim V_h=the number of vertices of $\mathcal{T}_h$) and where B_h is a $M_h \times N_h$ matrix (with M_h=dim Λ_h). Both matrices A_h and B_h have a very simple structure since:

1. matrix A_h is diagonal,
2. the entry b_{ij} of B_h is zero unless

$$\int_\gamma \theta_i w_j \, d\gamma \neq 0$$

where θ_i (resp., w_j) is the i^{th} (resp., j^{th}) basis function of Λ_h (resp., V_h); indeed most entries of B_h are zero.

From the above properties of A_h and B_h, the $M_h \times M_h$ matrix $B_h A_h^{-1} B_h^t$ is sparse, easy to compute and/or to invert; it is "located along γ". We can either compute it once for all and then compute its Cholesky factors or solve (4.16) by a Uzawa/conjugate gradient algorithm operating in $\boldsymbol{R}^{M_h}$.

Remark 4.1. Using energy techniques it is easy to show that scheme (4.12)-(4.15) to be stable has to satisfy a relation such as

$$\triangle t < ch \tag{4.17}$$

where, in (4.17), c is independent of γ. □

4.4 Numerical Experiments

We shall report in this paragraph the solution of three test problems by the fictitious domain method (briefly) discussed in previous three subsections. These problems are *two-dimensional* and concerned by the scattering of harmonic planar waves, such as $e^{i(\alpha t + \mathbf{k}\cdot\mathbf{x})}$ (with $|\mathbf{k}| = 2\pi/\lambda$, λ being the wave length), by *perfectly reflecting* obstacles, namely a *disk*, a *NACA0012 airfoil* and a *semi-open cavity*. For all these test problems the artificial boundary Γ has been located at a distance of 3 λ, at least, from the scattering obstacle. We time integrate system (4.1)-(4.4) until we reach periodic solution.

(i) *First Test Problem: Scattering by a disk*

If we uses the notation of Figure 10, the scattering obstacle ω is a disk of radius .25 meter. The frequency is .6 GHz, implying (since the speed of light is $c = 3 \times 10^8$ meter/sec.) that the wave length is .5 meter. We suppose that ω is "illuminated" by a wave coming from the left and propagating in the horizontal direction. Concerning discretization we have used a triangulation $\mathcal{T}_h$ consisting of 25,088 triangles and 12,769 vertices with $h = \lambda/16$. We have taken $\triangle t = T/25$ (with $T = 2\pi/\alpha$).

For the present test problem the exact solution is known when Γ is located at infinity, i.e., when $\Omega = \boldsymbol{R}^2$. On Figures 12 to 17 we have compared the exact and computed real and imaginary parts of the scattered wave; we have compared the values taken by the exact and computed solutions on the half-lines containing the center of ω and parallel to the incidence direction (Figures 12 and 13), opposite to the incidence direction (Figures 14 and 15) and orthogonal to the incidence direction (Figures 16 and 17). Further calculations (to be reported elsewhere) show that, for h and $\triangle t$ sufficiently small, the main source of error is the replacement of the original unbounded domain $\boldsymbol{R}^2 \setminus \bar{\omega}$ by a bounded computational one with (4.3) specified on the artificial boundary Γ. Indeed the error decreases if for h and $\triangle t$ sufficiently small the distance from Γ to ω increases.

(ii) *Second Test Problem: Scattering by a NACA0012 airfoil*

The obstacle is a NACA0012 airfoil. The frequency is 3 GHz, implying that $\lambda = .1$ meter. The length of the airfoil chord is 4λ. The airfoil is illuminated by a wave coming from the left with a 45° angle of incidence. The computational domain Ω is

the rectangle $(-.5, .5) \times (-.4, .4)$ shown on Figure 18 together with the triangulation $\mathcal{T}_h$ used for computation; $\mathcal{T}_h$ consists of 40,960 triangles and 20,769 vertices, with $h = \lambda/16$. Figure 19 shows a more detailed view of the mesh, close to the airfoil. For the time step we have used $\triangle t = T/25$. On Figures 20 and 21 we have represented the real and imaginary components of the *total* field. A shadow region clearly appears above the airfoil in the illumination direction.

(iii) *Third Test Problem: Scattering by a semi-open cavity*

For this test problem the obstacle Ω is a semi-open cavity like the one shown in Figure 22. We suppose that the frequency of the illuminating wave is 3 GHz, implying that $\lambda = .1$ meter. The illuminating wave is coming from the lower left of ω with a 30° angle of incidence. The internal length of ω is 4λ, its thickness is $\lambda/5$ and its external height is 1.4λ. On Figure 22 we have also shown part of the triangulation $\mathcal{T}_h$ used for the calculation: it consists of 60,384 triangles and 30,545 vertices. For our calculations we have used $h = \lambda/20$ and $\triangle t = T/50$. On Figures 23 and 24 we have represented the real and imaginary components of the scattered field, respectively.

5 Conclusion

Fictitious domain methods seem well suited to the numerical solution of linear and nonlinear partial differential equations of various types, associated to domains with curved boundaries. With respect to the methods discussed in this article we think that several further issues are worth investigating such as the speed up of the iterative methods described in this article and the use of higher order approximations in order to decrease the number of grid points.

Acknowledgements

We would like to acknowledge the helpful comments and suggestions of the following individuals: L. C. Cowsar, E. J. Dean, G. H. Golub, J. W. He, Y. Kuznetsov, W. Lawton, P. Le Tallec, J. Pasciak, M. Ravachol, P. Joly, J. Weiss, R. O. Wells, M. F. Wheeler, O. B. Widlund, and X. Zhou.

The support of the following corporations and institutions is acknowledged: AWARE, Dassault Aviation, INRIA, Texas Center for Advanced Molecular Computation, University of Houston, Université P. et M. Curie. We also benefited from the support of the NSF (Grants DMS 8822522, DMS 9112847, INT 8612680 and DMS 9217374), the Texas Board of Higher Education (Grants 003652156ARP and 003652146ATP), DRET (Grant 89424), DARPA (Contracts AFOSR F49620-89-C-0125 and AFOSR-90-0334) and again the NSF under the HPCC Grand Challenge Grant ECS-952.

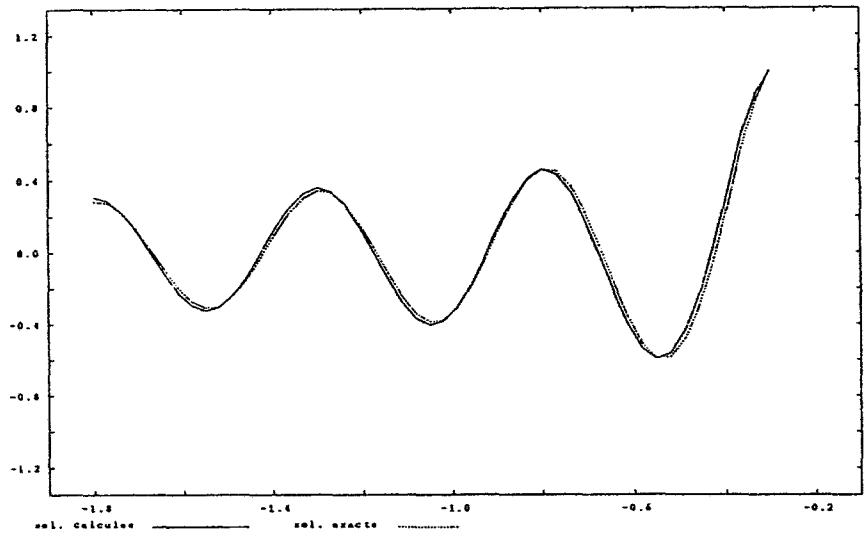

Figure 12

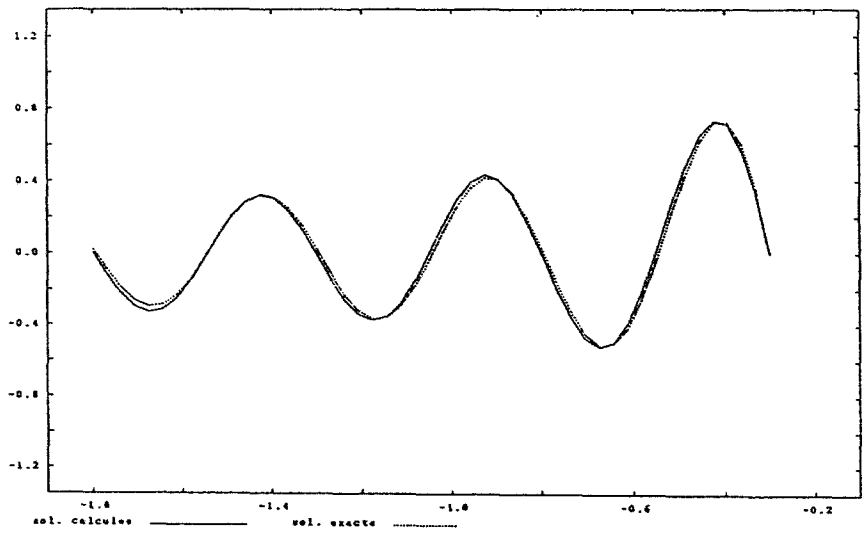

Figure 13

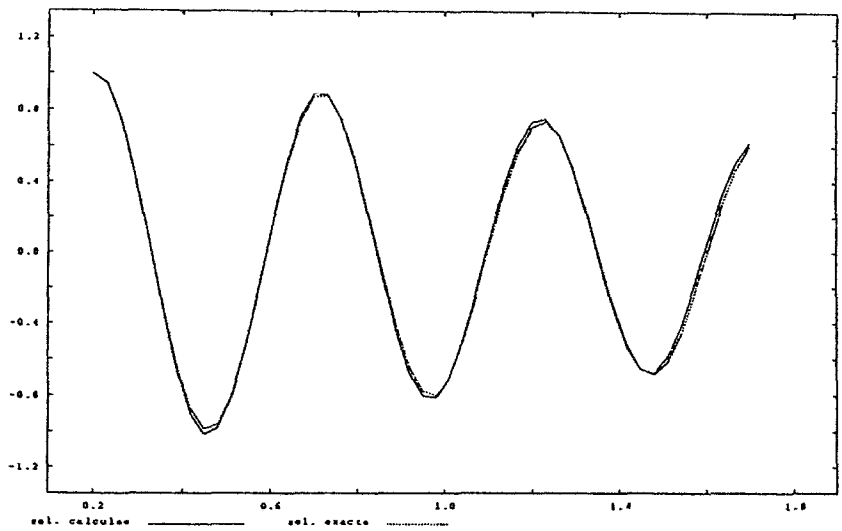

Figure 14

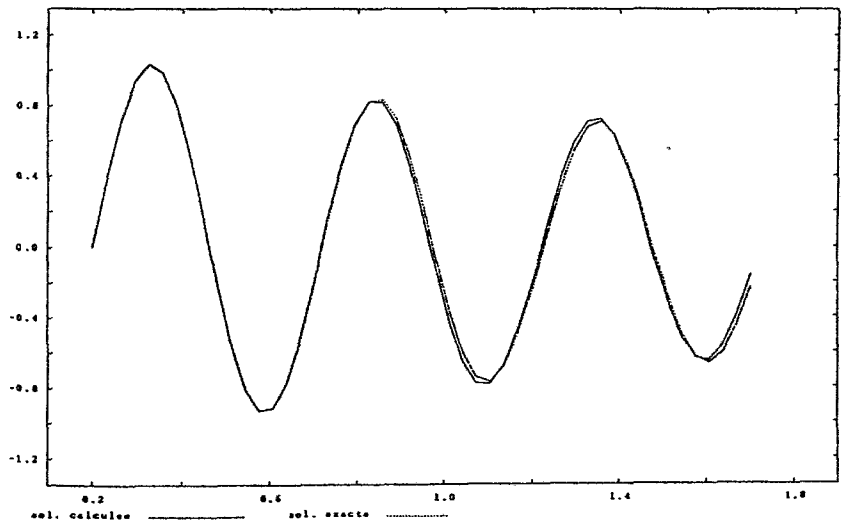

Figure 15

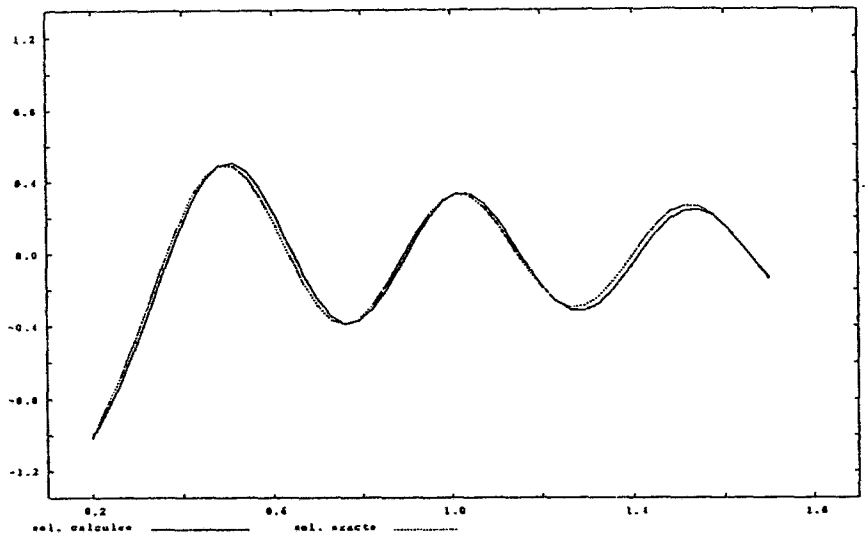

Figure 16

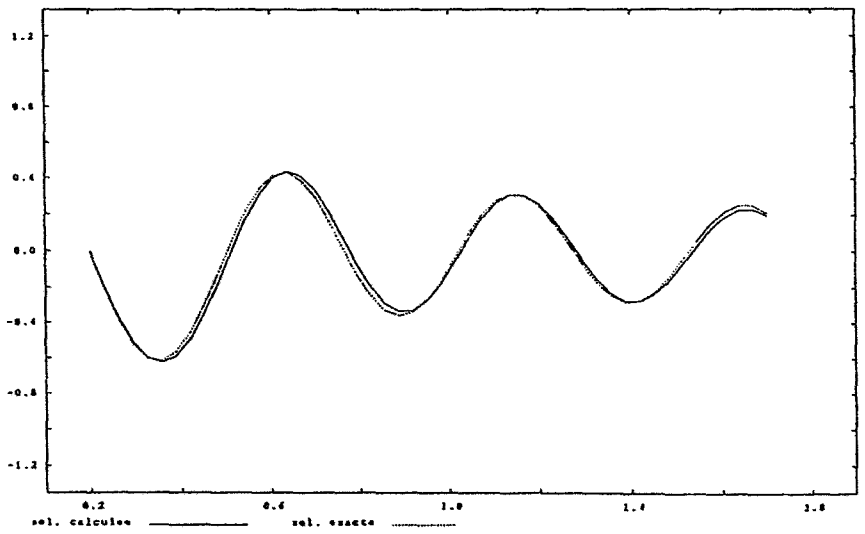

Figure 17

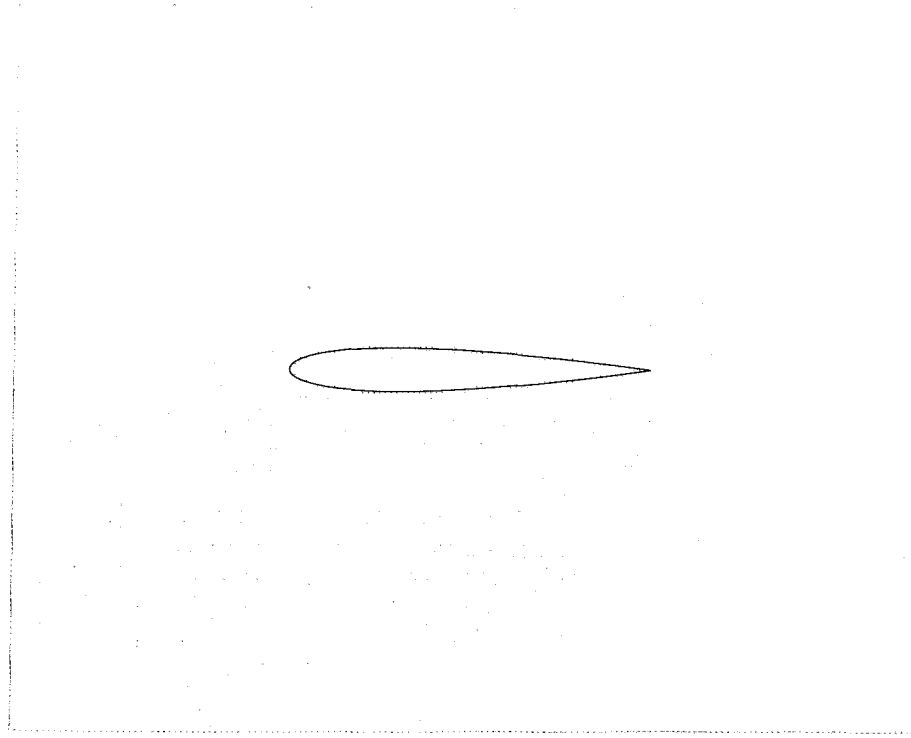

Figure 18

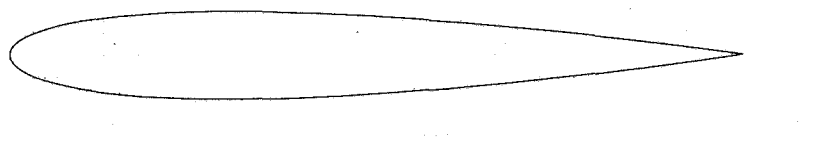

Figure 19

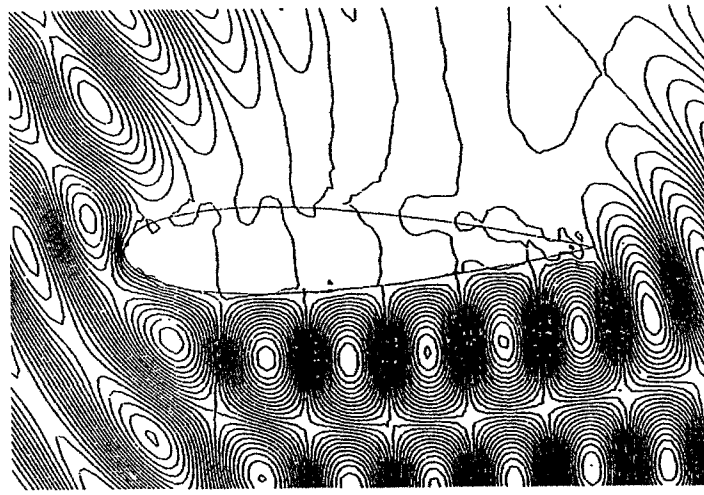

Figure 20

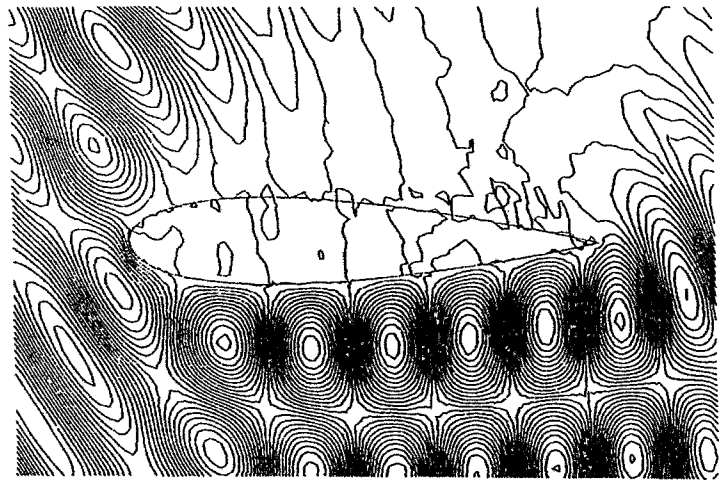

Figure 21

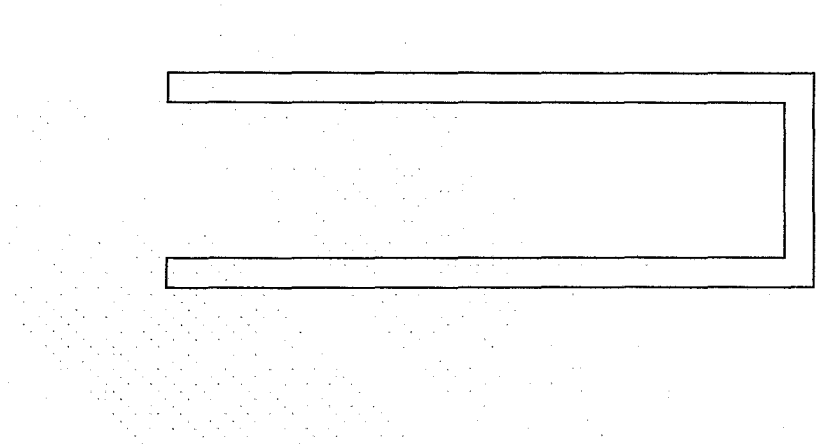

Figure 22

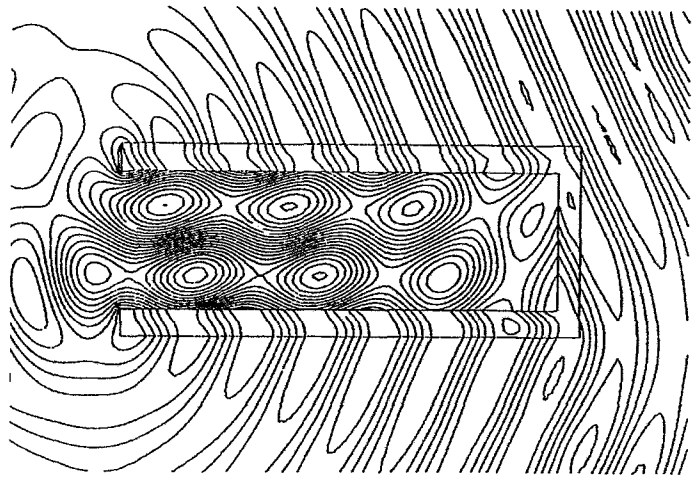

Figure 23

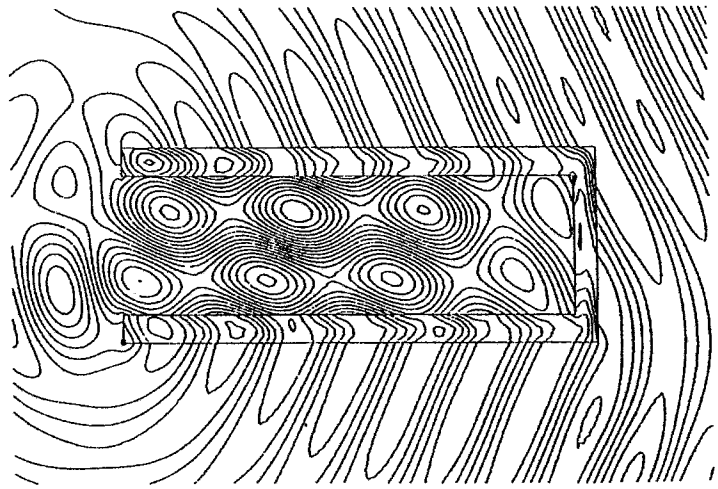

Figure 24

References

1. Proskurowski W., Widlund O. (1976) On the numerical solution of Helmholtz equation by the capacitance matrix method. *Math. Comp.*, 30: 433-468.
2. O'Leary D.P., Widlund O. (1979) Capacitance matrix methods for the Helmholtz equation on general three-dimensional regions. *Math. Comp.*, 33: 849-879.
3. Marchuk G.I., Kuznetsov Y.A., Matsokin A.M. (1986) Fictitious domain and domain decomposition methods. *Sov. J. Num. Anal. Math. Modeling*, 1: 3-35.
4. Finogenov S.A., Kuznetsov Y.A.(1988) Two-stage fictitious component methods for solving the Dirichlet boundary value problem. *Sov. J. Num. Anal. Math. Modeling*, 3: 301-323.
5. Glowinski R., Pan T.W., Periaux J. (1994) A fictitious domain method for Dirichlet problem and applications. *Comp. Meth. Appl. Mech. Eng.*, 111: 283-303.
6. Glowinski R., Pan T.W., Periaux J. (1994) A fictitious domain method for external incompressible viscous flow modeled by Navier-Stokes equations. *Comp. Meth. Appl. Mech. Eng.*, 112: 133-148.
7. Glowinski R., Pan T.W., Periaux J. (1995) A Lagrange multiplier/fictitious domain method for the Dirichlet problem. Generalization to some flow problems. *Japan J. of Industrial and Applied Mathematics*, 12: 87-108.
8. Glowinski R., Kearsley A.J., Pan T.W., Periaux J. (1995) Numerical simulation and optimal shape for viscous flow by fictitious domain method. *International J. for Numerical Methods in Fluids*, 20: 695-711.
9. Glowinski R. (1984) *Numerical methods for nonlinear variational problems*, Springer-Verlag, New York.
10. Girault V., Glowinski R. (1995) Error analysis of a fictitious domain method applied to a Dirichlet problem. *Japan J. of Industrial and Applied Mathematics*, 12: 487-514.
11. Glowinski R., Pan T.W., Periaux J. (1993) A one shot domain decomposition/fictitious domain method for the Navier-Stokes equations. In *Domain decomposition methods in scientific and engineering computing*, D.E. Keyes and J. Xu eds., AMS, Providence, RI, pp. 211-222.
12. Feng J., Joseph D.D., Glowinski R., Pan T.W. (1995) A three-dimensional computation on the force and moment on an ellipsoid settling slowly through a viscoelastic fluid. *J. of Fluid Mechanics*, 283: 1-16.
13. Bristeau M.O., Glowinski R, Periaux J. (1987) Numerical methods for the Navier-Stokes equations. Applications to the simulation of compressible and incompressible viscous flow. *Computer Phys. Rep.*, 6: 73-187.
14. Dean E.J., Glowinski R, Li C.H. (1989) Supercomputer solutions of partial differential equation problems in Computational Fluid Dynamics and in Control. *Computer Phys.*

Comm., 53: 401-439.
15. Glowinski R., Le Tallec P. (1989) *Augmented Lagrangian and operator splitting methods in nonlinear mechanics*, SIAM, Philadelphia.
16. Glowinski R. (1991) Finite element methods for the numerical simulation of incompressible viscous flow. Introduction to the control of the Navier-Stokes equations. In *Vortex Dynamics and Vortex Methods*, C.R. Andersonn and C. Greengard eds., Lectures in Applied Mathematics, **28**, AMS, Providence, R.I., pp. 219-301.
17. Marchuk G.I. (1990) Splitting and alternate direction methods. In *Handbook of Numerical Analysis, Vol. I*, P.G. Ciarlet and J.L. Lions eds., North-Holland, Amsterdam, pp. 197-462.
18. Glowinski R. (1985) Viscous flow simulation by finite element methods and related numerical techniques. In *Progress and Supercomputing in Computational Fluid Dynamics*, E. M. Murman and S. S. Abarbanel eds., Birkhauser, Boston, pp. 173-210.
19. Glowinski R. (1986) Splitting methods for the numerical solution of the incompressible Navier-Stokes equations. In *Vistas in Applied Mathematics*, A.V. Balakrishnan, A.A. Dorodnitsyn and J.L. Lions, eds., Optimzation Software, New York, pp. 57-95.
20. Kuznetsov Y.A., Wheeler M.F. (1995) Optimal order substructuring preconditioners for mixed finite element on nonmatching grids. *East-West J. of Num. Math.*, 3: 127-143.